

# Theoretical design of coupled high contrast grating (CHCG) waveguides to enhance $\text{CO}_2$ light-absorption for gas sensing applications

Cite as: J. Appl. Phys. **125**, 154502 (2019); <https://doi.org/10.1063/1.5091933>

Submitted: 06 February 2019 . Accepted: 29 March 2019 . Published Online: 18 April 2019

Tahere Hemati , and Binbin Weng 



View Online



Export Citation



CrossMark

Applied Physics Reviews  
Now accepting original research

2017 Journal  
Impact Factor:  
**12.894**

AIP  
Publishing

# Theoretical design of coupled high contrast grating (CHCG) waveguides to enhance CO<sub>2</sub> light-absorption for gas sensing applications

Cite as: J. Appl. Phys. **125**, 154502 (2019); doi: [10.1063/1.5091933](https://doi.org/10.1063/1.5091933)

Submitted: 6 February 2019 · Accepted: 29 March 2019 ·

Published Online: 18 April 2019



Tahere Hemati and Binbin Weng<sup>a)</sup>

## AFFILIATIONS

School of Electrical and Computer Engineering, University of Oklahoma, Norman, Oklahoma 73019, USA

<sup>a)</sup>Electronic mail: [binbinweng@ou.edu](mailto:binbinweng@ou.edu)

## ABSTRACT

In this work, we present a theoretical study on using high contrast grating (HCG) designs to enhance light–gas interaction in the mid-infrared range. The optical behavior of a single layer HCG was studied under the presence of CO<sub>2</sub> gas. Through optimizing the structure parameters, we could confine an intense electric field over the grating layer. Consequently, about 200 times of light-absorption enhancement was observed. To further improve the performance, a coupled HCG (CHCG) was proposed to introduce another vertical photonic confinement mechanism. We found that CHCG can restrict much intense light energy in the structure leading to over 600 times of light-absorption enhancement. However, it is noticed that a significant part of the concentrated electric field was still trapped in the high index areas, where the gas cannot interact. To address this issue, a modified CHCG with a thin substrate thickness was proposed. Through the optimization ( $T = 1.149\ \mu\text{m}$ ), we were able to redistribute most of the light energy into the void space of the CHCG layer which resulted in close to 1400 times of improvement. This work clearly demonstrates that using HCG for enhancing light–gas interaction is a promising approach to make on-chip gas sensing devices. Furthermore, it can also be integrated into other photonic components, e.g., fibers for advanced sensing system development.

Published under license by AIP Publishing. <https://doi.org/10.1063/1.5091933>

## I. INTRODUCTION

Gas sensing has a variety of vital applications in environmental monitoring,<sup>1</sup> disease diagnosis,<sup>2</sup> manufacturing control,<sup>3</sup> and national security surveillance.<sup>4</sup> Among different sensing methods, mostly thanks to advanced nanofabrication technology, chip-scale photonic-based sensors have received increasing attention. They offer multiple advantages, including faster response, higher sensitivity, compact size, low power consumption, and relatively low cost.<sup>5</sup> These properties make them a competitive candidate to be used for many newly emerging technologies, such as the Internet of Things (IoTs). High contrast grating (HCG) photonic technology will lead to the development of a lab-on-chip small, low-power, and low-cost gas sensing device. Such devices can be integrated into current mobile devices and generate sensing data that can be shared on the internet simultaneously. As such, the presented work will be highly beneficial to the fast-developing IoT infrastructure.<sup>6</sup>

Generally, photonic-based sensing technologies can be categorized into two groups: (1) refractive index-based<sup>7,8</sup> and (2) absorption-based.<sup>9,10</sup> In refractive index-based sensors, by

introducing a gas or a liquid to a photonic structure, the refractive index changes, and thus the spectrum resonant peak of reflected or transmitted light shifts. Through measuring the shifted value, the gas can be detected.<sup>11</sup> This sensor is sensitive to small changes in the refractive index of the surrounding medium. However, since gas species and the concentration factors can both affect refractive index values, distinguishing between different gases can be challenging.<sup>12</sup>

Fortunately, this issue can be addressed by the absorption-based method. Due to the intrinsic molecular vibration modes, the selectivity can be improved. As light passes through an analyte, the reflection or transmission is attenuated at specific wavelengths, due to molecule absorptions, which are unique for each gas species. Increasing the gas concentration leads to an increased attenuated value.<sup>13</sup> Nevertheless, to achieve proper sensitivity in the absorption-based approach, we need to increase the light–matter interaction. Traditionally, this goal was attained by increasing the interaction path which led to the fabrication of large and costly devices. Fortunately, in recent years, significant progress in the nanofabrication technology has inspired a significant number of scholars to

introduce new photonic structures<sup>14–18</sup> to increase the light–matter interaction without extending the interaction path.

Among different microsize structures, simplicity and effectiveness of gratings have drawn significant attention toward HCGs for sensing applications. Gratings have been widely used in refractive index-based sensors.<sup>17,19–22</sup> However, very few works have been reported on using this structure in absorption-based sensors.<sup>23</sup> Normally, light tends to be confined to high index areas. This tendency can make the grating optimization challenging for absorption-based gas sensors.

In this work, we aim to combine HCGs and the absorption-based method to investigate the light–matter interaction in the mid-infrared range. Here, our test sample is CO<sub>2</sub> because of its significant impacts on environmental, medical,<sup>24</sup> and industrial<sup>25</sup> areas. The calculated absorption coefficient for 1% of CO<sub>2</sub>, around 4.3 μm (the signature line absorption of CO<sub>2</sub> in the mid-IR range), was reported to be 0.3 cm<sup>-1</sup> Pa<sup>-1</sup>.<sup>26</sup> It should be mentioned that by adjusting grating parameters of the CHCG photonic structure, the technology can be applied for detecting other gases as well.

## II. NUMERICAL DESIGN, DISCUSSION, AND RESULTS

In this section, by using rigorous coupled-wave analysis (RCWA) method, the functionality of the single high contrast grating (SHCG) and CHCG in enhancing light-absorption of CO<sub>2</sub> will be studied. RCWA is a well-known numerical method used to solve Maxwell's equations and to analyze the transmitted, reflected, and absorbed waves from a planar grating restricted by two materials with different refractive indices.<sup>27,28</sup> Effective parameters in the grating design are grating thickness, air gap thickness, fill factor, and the period which are optimized accurately in this study. Lastly, it is noted that our numerical design is based on TE polarized modes, simply because light wave of TE modes has a much larger spatial coupling volume with gas molecules which could lead to an enhanced gas sensing performance. Specifically, when electromagnetic (EM) field reaches to a dielectric boundary, TM modes tend to stay in high index areas because its nodal plane presents at the boundary which expels the EM displacement field back to the high index areas.<sup>29</sup> However, such nodal plane for TE modes does not exist at the boundary which allow the energy penetration into the lower dielectric area having gas molecules.<sup>30–32</sup>

### A. Single HCG (SHCG)

The schematic view of the SHCG consisting of a grating layer of silicon ( $n_{\text{Si}} = 3.5$ ) and a layer of SiO<sub>2</sub> ( $n_{\text{SiO}_2} = 1.4$ ) as a substrate is illustrated in Figs. 1(a) and 1(b). The design parameters, including the grating layer thickness  $D_1$ , fill factor  $F$ , and grating period  $\Lambda$  are indicated. Through optimizing the grating parameters, we aim to restrict an intense light over the grating layer of the SHCG.

In this way, we are able to increase the chance of interaction of light and the gas which leads to enhanced light-absorption phenomena. Besides, it is expected that by increasing electric field intensity, the value of enhancement increases as well. Moreover, as much as we could trap the light in low index areas over the grating layer, we will have more effective light–matter interaction. However, due to the tendency of light to be confined in the high index area, the optimization process by using SHCG can be challenging.

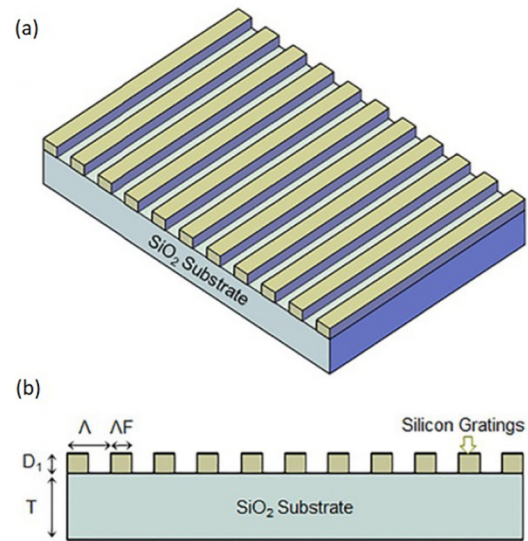


**FIG. 1.** (a) A 3D schematic view of the SHCG, made of silicon with the SiO<sub>2</sub> substrate (relative to the grating thickness, the substrate thickness is infinite). (b) The cross-sectional view of the SHCG. The grating layer thickness  $D_1$ , the fill factor  $F$ , and the grating period  $\Lambda$  are demonstrated in the figure.

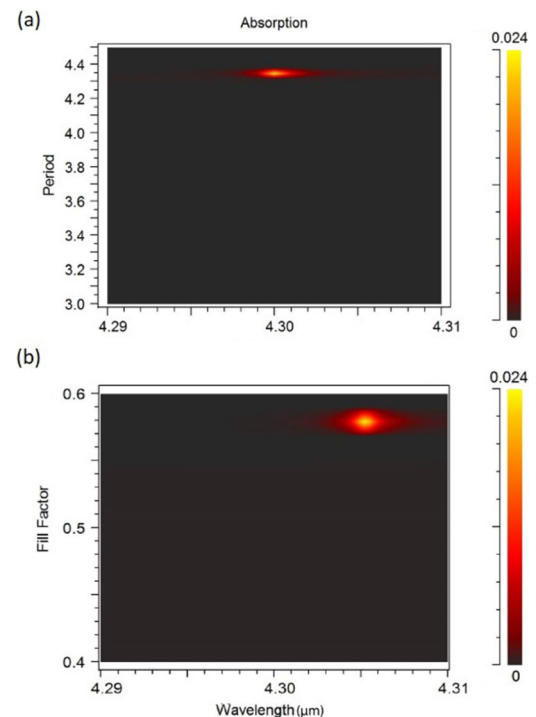


**FIG. 2.** (a) Changing pattern of the light absorption given by manipulating the period. The optimized period  $\approx 4.3 \mu\text{m}$ . (b) Changing pattern of the light absorption given by manipulating the fill factor. The optimized fill factor  $\approx 0.57$ .

One of the most effective parameters in the grating optimization is the grating period. According to the grating period, the optical gratings can be categorized into three regimes: (1) diffraction regime (the period is greater than the wavelength),<sup>33</sup> (2) deep-subwavelength regime (the period is much less than the wavelength),<sup>34</sup> and (3) near-wavelength regime (the period is almost equal to the wavelength). In the third regime, gratings behave entirely differently and show unusual features such as a broadband high-reflectivity<sup>35</sup> and the high-quality-factor resonance<sup>36</sup> in which the later one can lead to enhanced light-matter interaction. Hence, we selected the initial value of the period equal to  $4.3\ \mu\text{m}$ .

The other notable design parameter is the grating thickness. According to the incident light wavelength and the grating size, several waveguide modes are excited. These modes propagate through the grating and accumulate different phases. Due to the extreme mismatch between these modes and the exit plane, modes not only reflect but also couple to each other. The grating thickness defines the phase accumulated by the modes and controls their interference.<sup>37</sup> Hence, to achieve a high-quality-factor resonator, we need to choose the grating thickness such that at the exit and input planes a constructive interference is obtained.

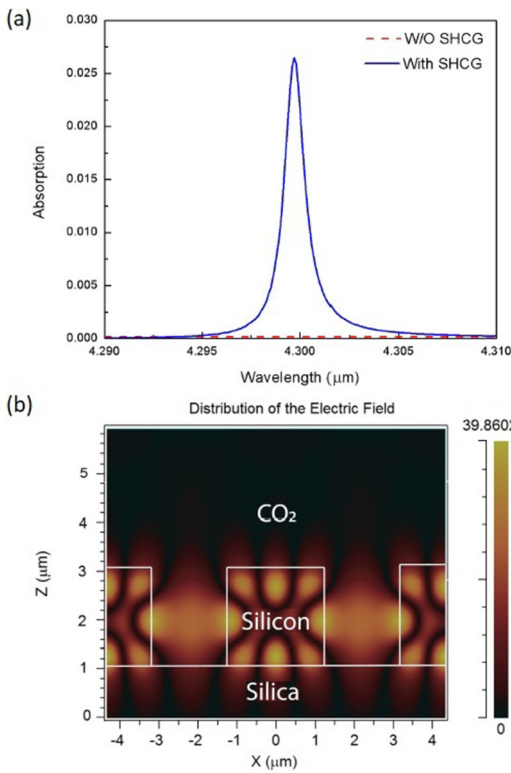


**FIG. 3.** (a) The absorption spectra of  $\text{CO}_2$  with and without SHCG from  $4.29\ \mu\text{m}$  to  $4.31\ \mu\text{m}$  ( $\Lambda = 4.336\ \mu\text{m}$ ,  $F = 0.5775$ , and  $D_1 = 1.832\ \mu\text{m}$ ). The bandwidth of absorption peak =  $1.2\ \text{nm}$ . (b) The intensity and distribution of the confined electric field at  $4.3\ \mu\text{m}$  on the SHCG. The colored bar shows the intensity of the electric field  $(\text{V}/\mu\text{m})^2$ .

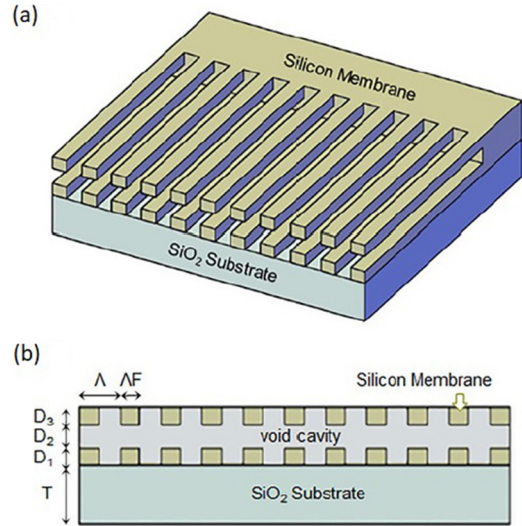


**FIG. 4.** (a) A 3D schematic view of the CHCG, made of silicon with  $\text{SiO}_2$  substrate. (b) The cross sectional view of the HCG. The bottom grating layer thickness  $D_1$ , the air gap thickness  $D_2$ , the top grating layer thickness  $D_3$ , the substrate thickness  $T$ , the fill factor  $F$ , and the grating period  $\Lambda$  are shown in the figure. This structure is supposed to be located in the gas chamber.

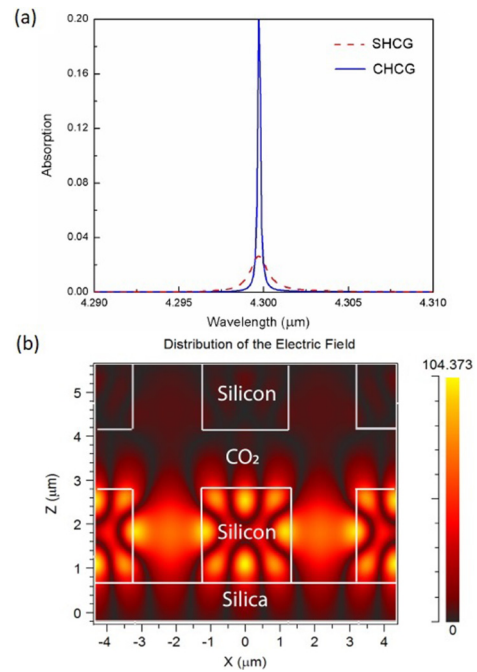


**FIG. 5.** (a) The absorption spectra of  $\text{CO}_2$  with and without CHCG from  $4.29\ \mu\text{m}$  to  $4.31\ \mu\text{m}$ ;  $D_1 = 1.832\ \mu\text{m}$ ,  $D_2 = 1.14\ \mu\text{m}$ ,  $D_3 = 1.55\ \mu\text{m}$ ,  $T = \text{infinite}$ ,  $\Lambda = 4.336\ \mu\text{m}$ , and  $F = 0.5775$ . The bandwidth of absorption peak =  $0.25\ \text{nm}$ . (b) The intensity and distribution of the confined electric field at  $4.3\ \mu\text{m}$  on the CHCG. The colored bar shows the intensity of the electric field  $(\text{V}/\mu\text{m})^2$ .

In order to achieve strong light absorption at the wavelength matching with the  $\text{CO}_2$  vibration mode, grating parameters of the HCG structure needs to be modified and optimized. The rule of thumb for the design is to establish constructive light waves in the void low refractive index areas where gas molecules exist.<sup>38</sup> In this way, the strong resonating light energy will be able to spatially couple with gas molecules effectively. Figures 2(a) and 2(b) show the optimized value of the grating period  $\approx 4.3\ \mu\text{m}$  and fill factor  $\approx 0.57$  around  $4.3\ \mu\text{m}$ , where the absorption has its highest

value. The color in these figures indicates the light-absorption strength. From dark black to bright yellowish color, the intensity of the absorption increases. Clearly, it is shown that a strong light absorption can be achieved with an optimized grating period and fill factor. On the contrary, without any optimization, the absorption effect can barely be obtained in the grating structure. The same process is done to optimize the grating thickness. It is necessary to mention that all optimization parameters are correlated with each other, changing one parameter changes the other.

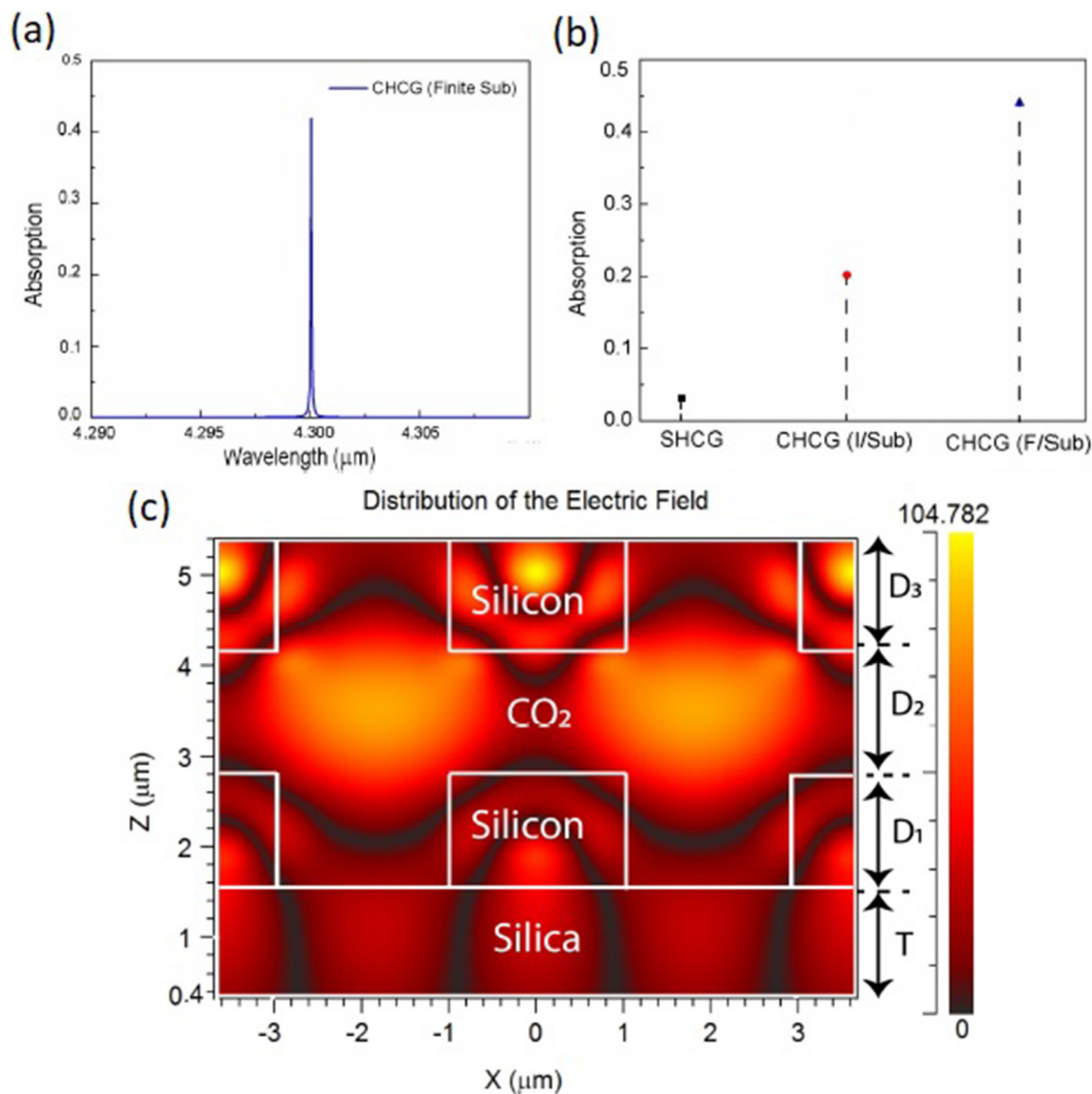


**FIG. 6.** (a) The absorption spectra of  $\text{CO}_2$ , given by optimization CHCG with a finite substrate, from  $4.29\ \mu\text{m}$  to  $4.31\ \mu\text{m}$   $D_1 = 0.99\ \mu\text{m}$ ,  $D_2 = 1.15\ \mu\text{m}$ ,  $D_3 = 1.215\ \mu\text{m}$ ,  $T = 1.149\ \mu\text{m}$ ,  $\Lambda = 3.6378\ \mu\text{m}$ , and  $F = 0.5325$ . The bandwidth of absorption peak =  $0.1\ \text{nm}$ . (b) A comparison between the absorption value of SHCG, CHCG with infinite substrate, and CHCG with finite substrate. (c) The intensity and distribution of the confined electric field at  $4.3\ \mu\text{m}$  on the CHCG with the finite substrate. The colored bar shows the intensity of the electric field  $(\text{V}/\mu\text{m})^2$ .

Thus, this correlation makes the optimization process challenging and time-consuming.

The given absorption spectra of CO<sub>2</sub>, via the grating optimization ( $\Lambda = 4.336\mu\text{m}$ ,  $F = 0.5775$ , and  $D_1 = 1.832\mu\text{m}$ ) is shown in Fig. 3(a). While the absorption value of CO<sub>2</sub> without the HCG is approximately  $10^{-4}$ , the implementation of the optimized SHCG enhanced this value to  $\approx 2 \times 10^{-2}$ . This improvement ( $\sim 200$  times) is emanated from confining the intense electric field to the grating layer. The intensity and distribution of the electric field at  $4.3\mu\text{m}$  are demonstrated in Fig. 3(b). It is evident that if we can confine more intense electric field over the grating layer, we will have more efficient light-matter interaction. Thus, in Sec. II B, we propose a new coupled HCG (CHCG) design in order to add in another vertical optical confinement for concentrating more light energy in the device.

### B. Coupled HCG (CHCG)

Designing a new HCG layer with the same period and fill factor but different thickness, and coupling this new layer with the previous one to make a gap between them, gives us two more parameters to optimize air gap thickness ( $D_2$ ) and the thickness of new HCG ( $D_3$ ). Figures 4(a) and 4(b) show a 3D and a cross-sectional view of CHCG, respectively. In the simulation, a similar optimizing strategy was used for these two new grating parameters.

Compared to Fig. 3(b), this design, through confining a more intense electric field ( $\approx 2.5$  times stronger), as shown in Fig. 5(b), gave us roughly 600 times enhancement. As demonstrated in Fig. 5(a), the maximized absorption value of CO<sub>2</sub> increased from 0.025 in SHCG to 0.2 in the CHCG. Although the intense electric field has not been confined completely in grooves, where CO<sub>2</sub> exists, this amount of confinement could still lead to such improved absorption enhancement. Therefore, it is expected that it could lead to even further improvement. Later on, we found that through optimizing the substrate thickness  $T$ , which had been considered infinite so far, we could trap the light mostly in low index areas. Our suggested explanation is that adjusting the thickness of the SiO<sub>2</sub> substrate provides us an additional tuning factor to further improve light confinement or the waveguiding effect in the vertical direction, which leads to a strong constructive resonating effect that infinite substrate cannot provide.

### C. Modified CHCG

Figures 6(a) and 6(b) show the absorption spectrum of the new CHCG design and a comparison between the enhanced absorption value of the SHCG, the CHCG with infinite substrate, and the CHCG with finite substrate. In this new design, we optimized the substrate (the most bottom layer on which added layers are mounted) thickness. Through this new design ( $D_1 = 0.99\mu\text{m}$ ,  $D_2 = 1.15\mu\text{m}$ ,  $D_3 = 1.215\mu\text{m}$ ,  $T = 1.149\mu\text{m}$ ,  $F = 0.5325$ ,  $\Lambda = 3.6378\mu\text{m}$ ), we could increase the absorption value to 1400 times of its initial value where there was no HCG. Figure 6(c) shows clearly the origin of this value of enhancement which comes from trapping the intense electric field mostly in the gap between two grating layers. It should be mentioned that, although the fabrication of such a thin substrate is challenging, it is fortunately still possible, due to advanced current technologies.

### III. CONCLUSION

To conclude, we presented a theoretical approach to enhance light absorption by an increased light-matter interaction for CO<sub>2</sub> gas sensing applications. To attain this goal, we benefited from unique properties of CHCGs for localizing an intense electric field in the gap between the two grating layers. In this study, we demonstrated the advantage of CHCGs and TE modes in confining the light respect to a single layer of HCG. Hence, compared to SHCG, the optimized CHCG can increase the light absorption by seven times. Generally, by utilization of the optimized CHCGs, which enables us to trap more intense light over the grating layer, we could increase the absorption value from  $3 \times 10^{-4}$  to 0.2. In other words, we improved the light absorption by 600 times. Finally, through optimizing the substrate thickness, we could confine the intense electric field mostly to low index areas which led to more effective light-matter interaction and 1400 times of light-absorption enhancement. Our study demonstrated the capability of CHCGs in enhancing the light absorption in the microsize level and introduced a promising candidate for a new generation of on-chip absorption-based detectors which can be integrated to other photonic components in the future.

### REFERENCES

- 1C. Fischer, M. Sigrist, Q. Yu, and M. Seiter, *Opt. Lett.* **26**, 1609 (2001).
- 2B. Buszewski, M. Kęsy, T. Ligor, and A. Amann, *Biomed. Chromatogr.* **21**, 553 (2007).
- 3J. Riegel, H. Neumann, and H.-M. Wiedenmann, *Solid State Ionics* **152**, 783 (2002).
- 4T. Hemati and B. Weng, "The mid-infrared photonic crystals for gas sensing applications," in *Photonic Crystals—A Glimpse of the Current Research Trends* (IntechOpen, 2018).
- 5J. Hodgkinson and R. P. Tatam, *Meas. Sci. Technol.* **24**, 012004 (2012).
- 6D. Blaauw, D. Sylvester, P. Dutta, Y. Lee, I. Lee, S. Bang, Y. Kim *et al.*, "IoT design space challenges: Circuits and systems," in *2014 Symposium on VLSI Technology (VLSI-Technology): Digest of Technical Papers* (IEEE, 2014).
- 7M. Quan, J. Tian, and Y. Yao, *Opt. Lett.* **40**, 4891 (2015).
- 8L. Wang, T. Sang, J. Li, J. Zhou, B. Wang, and Y. Wang, *J. Mod. Opt.* **65**, 1–8 (2018).
- 9J. Wang and L. Wang, *Opt. Lett.* **35**, 3270 (2010).
- 10W. Y. Peng, C. S. Goldenstein, R. M. Spearrin, J. B. Jeffries, and R. K. Hanson, *Appl. Opt.* **55**, 9347 (2016).
- 11A. Liu, W. H. E. Hofmann, and D. H. Bimberg, *IEEE J. Quantum Electron.* **51**, 1 (2015).
- 12G. Korotcenkov, *Handbook of Humidity Measurement, Volume 1: Spectroscopic Methods of Humidity Measurement* (CRC Press, 2018).
- 13U. Platt and J. Stutz, "Differential absorption spectroscopy," in *Differential Optical Absorption Spectroscopy* (Springer, 2008), pp. 135–174.
- 14V. Selvakumar, L. Sujatha, and R. Sundar, *Sens. Lett.* **16**, 188 (2018).
- 15D. Pergande, T. M. Geppert, A. v. Rhein, S. L. Schweizer, R. B. Wehrspohn, S. Moretton, and A. Lambrecht, *J. Appl. Phys.* **109**, 083117 (2011).
- 16A. K. Goyal, H. S. Dutta, and S. Pal, *J. Phys. D Appl. Phys.* **50**, 203001 (2017).
- 17M. Marciniak, M. Gębski, M. Dems, and T. Czystanowski, *Politechnika Łódzka* **38**, 1219 (2017).
- 18S. Zheng, M. Ghandehari, and J. Ou, *Sens. Actuators B* **223**, 324 (2016).
- 19X. Wei and S. M. Weiss, *Opt. Express* **19**, 11330 (2011).
- 20K. Li, N. Zhang, N. M. Y. Zhang, G. Liu, T. Zhang, and L. Wei, *Opt. Lett.* **43**, 679 (2018).
- 21Á. González-Vila, A. Ioannou, M. Loyez, M. Debliquy, D. Lahem, and C. Caucheteur, *Opt. Lett.* **43**, 2308 (2018).

- <sup>22</sup>K. Tiefenthaler and W. Lukosz, *Thin Solid Films* **126**, 205 (1985).
- <sup>23</sup>Y. Wu, B. Yao, A. Zhang, Y. Rao, Z. Wang, Y. Cheng, Y. Gong, W. Zhang, Y. Chen, and K. Chiang, *Opt. Lett.* **39**, 1235 (2014).
- <sup>24</sup>M. Folke, L. Cernerud, M. Ekström, and B. Hök, *Med. Biol. Eng. Comput.* **41**, 377 (2003).
- <sup>25</sup>S. Neethirajan, D. Jayas, and S. Sadistap, *Food Bioprocess. Technol.* **2**, 115 (2009).
- <sup>26</sup>K. Wakatsuki, S. P. Fuss, A. Hamins, and M. R. Nyden, *Proc. Combust. Inst.* **30**, 1565 (2005).
- <sup>27</sup>M. Moharam, E. B. Grann, D. A. Pommet, and T. Gaylord, *J. Opt. Soc. Am. A* **12**, 1068 (1995).
- <sup>28</sup>T. Hemati and B. Weng, *J. Appl. Phys.* **124**, 053105 (2018).
- <sup>29</sup>J. D. Joannopoulos, S. G. Johnson, J. N. Winn, and R. D. Meade, *Molding the Low of Light* (Princeton University Press, Princeton, NJ, 2008).
- <sup>30</sup>V. R. Almeida, Q. Xu, C. A. Barrios, and M. Lipson, *Opt. Lett.* **29**, 1209 (2004).
- <sup>31</sup>M.-C. Tien, J. F. Bauters, M. J. Heck, D. T. Spencer, D. J. Blumenthal, and J. E. Bowers, *Opt. Express* **19**, 13551 (2011).
- <sup>32</sup>O. Painter, J. Vučković, and A. Scherer, *J. Opt. Soc. Am. B* **16**, 275 (1999).
- <sup>33</sup>E. G. Loewen and E. Popov, *Diffraction Gratings and Applications* (CRC Press, 1997).
- <sup>34</sup>B. C. Kress and P. Meyrueis, *Applied Digital Optics: From Micro-Optics to Nanophotonics* (John Wiley & Sons, 2009).
- <sup>35</sup>C. F. Mateus, M. C. Huang, Y. Deng, A. R. Neureuther, and C. J. Chang-Hasnain, *IEEE Photonics Technol. Lett.* **16**, 518 (2004).
- <sup>36</sup>D. Rosenblatt, A. Sharon, and A. A. Friesem, *IEEE J. Quantum Electron.* **33**, 2038 (1997).
- <sup>37</sup>C. J. Chang-Hasnain and W. Yang, *Adv. Opt. Photonics* **4**, 379 (2012).
- <sup>38</sup>W. P. Huang, *J. Opt. Soc. Am. A* **11**, 3 (1994).